DESIGN OF NEURAL NETWORKS ALGORITHMS FOR THE RETRIEVAL OF TROPOSPHERIC OZONE FROM SATELLITE DATA

F. Del Frate, P. Sellitto, and D. Solimini

Earth Observation Laboratory, DISP, Tor Vergata University of Rome, Mailing address: DISP Building DT-09, Via del Politecnico 1, 00133, Rome, ITALY, Email contact: sellitto@disp.uniroma2.it

ABSTRACT

This paper reports on the development of Neural Networks algorithms for tropospheric ozone retrieval from ESA-Envisat SCIAMACHY measurements. We present and discuss some retrieval experiments from UV/VIS simulated data, based upon a combined sensitivity analysis performed with the aid of the UVSPEC radiative transfer model and a neural Extended Pruning procedure. In particular, the role of UV and VIS information budget is here exploited and critically discussed.

Key words: tropospheric ozone, neural networks, air pollution.

1. INTRODUCTION

Inferring tropospheric ozone information from satellite nadir data is a difficult task owing to the poor sensitivity of the Earth's radiance to ozone variations in the atmospheric lower levels. Most of the existing techniques to retrieve information about the ozone in troposphere from space are based on Tropospheric Ozone Residual (TOR) methodology, that is, stratospheric ozone, measured eventually by a limb viewing sensor, is subtracted from the total column ozone content, measured eventually by a nadir viewing instrument [1, 2, 3]. Another indirect method relies with the integration of the tropospheric concentration of ozone from pre-inferred ozone profiles [4, 5]. However, a direct technique, referring only to nadir measurements, could be more effective because 1) it requires only data from one instrument, and 2) it would be possible, ideally, to obtain better horizontal resolutions. Experience on ESA-ERS2 GOME data demonstrated the suitability of Neural Networks (NNs) schemes as an alternative method to obtain ozone information with less time and computational efforts [6, 7, 8, 9]. NNs are composed of some computational elements called neurons, linked with weighted synapses. In the training phase, the NN learns the mapping between input and output vectors by optimizing the synapses' weights. It has been demonstrated that, providing that the learning dataset is representative of the phenomena to be modelled and a sufficient number of processing units is considered, NNs, in particular Multi Layer Perceptrons, can approximate any continuous mapping function with the desired accuracy [10].

In this paper we first present the results obtained by a sensitivity study performed with the LibRadtran suite [11]. The study aims at exploring the relative information budget in UV and VIS spectral ranges, in relation to tropospheric sounding. Secondly we report on the performance of the subsequently designed Neural Networks algorithms, specifically dedicated to tropospheric ozone retrievals from simulated ENVISAT-SCIAMACHY radiance spectra.

2. HEIGHT RESOLVED SENSITIVITY STUDY OF THE EARTH'S UV/VIS RADIANCE TO TROPOSPHERIC OZONE VARIATIONS

To investigate the possibilities and limits of inferring the tropospheric ozone variations from satellite data we analyzed the variations in Earth's radiance resulting from changes of ozone concentration at different tropospheric heights. We used the UVSPEC radiative transfer model and the LibRadtran libraries to represent a summer mid-latitude urban environment. We selected the atmospheric state by choosing vertical profiles of air density, pressure and temperature, and ozone, oxygen, water vapor, carbon dioxide and nitrogen dioxide concentrations as in AFGL midlatitude summer climatological standard. The tropopause has been considered in the range 14-17 km. Aerosols optical properties were set as in standard state, and the absorption lines of the active species have been modelled with a Correlated K band parametrization. The solar spectrum was chosen at a resolution of 0.05 nm (*ATLAS PLUS MODTRAN* spectrum) and then interpolated at the operating wavelength of SCIAMACHY sensor in the interval 220-800 nm. The solar zenith angle (sza) has been put at a fixed value of 30° (mean value of sza at Rome station overpass), and observation geometry has been put as an exact nadir measurement (zenith and azimuth angles equal to 0). The SCIAMACHY sensor has been three fold modelled: a) the model was forced to solve the radiation transfer equation at the operating

Proc. 'Envisat Symposium 2007', Montreux, Switzerland
23–27 April 2007 (ESA SP-636, July 2007)

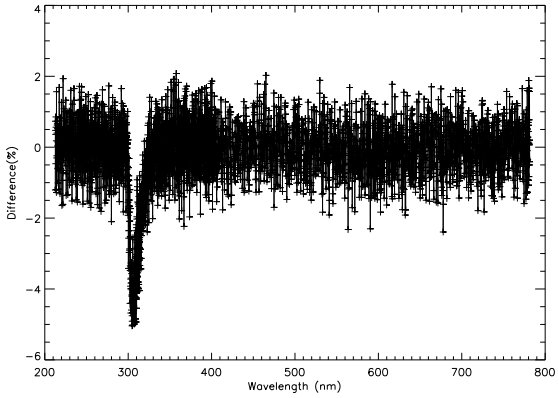

Figure 1. Spectral differences (%) of Earth's radiance for a doubling of ozone concentration at z=14 km with respect to standard AFGL midlatitude summer.

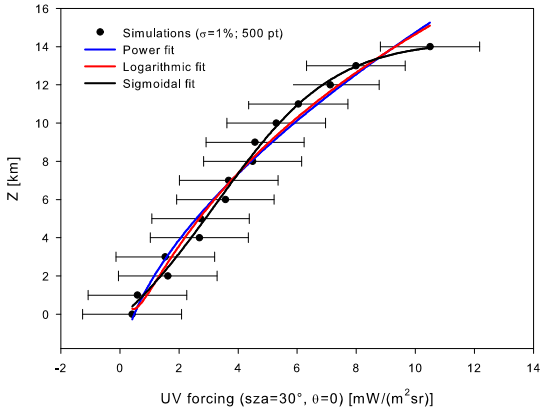

Figure 2. Dependence of UV radiative forcing at fixed observation angle for ozone doubling, with height. Some fitting functions are also represented. For sigmoidal fit $R^2 = 0.99$.

SCIAMACHY wavelengths, b) a Gaussian slit function with a FWHM = 0.3 nm was imposed to simulate the sensor's spectral resolution, and 3) a 1% level noise was added to the modelled radiances. Starting from these assumptions, the ozone concentrations were systematically enhanced at the tropospheric heights (0-14 km in our case) and the changes in backscattered UV/VIS spectra were analyzed. Figure 1 shows the differences (%) of Earth's radiance in the spectral range 220-800 nm, for a doubling of ozone at 14 km with respect to the standard case. Similar behaviors are reported for a doubling at each of the tropospheric heights; the maximum sensitivity is in the range 302-307 nm, mainly due to total ozone variations. A little sensitivity is also reported in the VIS range (around the interval 550-650 nm, in the Chappuis bands). To test the overall tropospheric information budget, we performed an integration of the mentioned differences in the sensible UV and VIS intervals for enhancements at each height level, calculating some sort of UV and VIS radiative forcing at fixed observation angle. The trends of these quantities are reported in figures 2 and 3. Figure 2 shows also the fitting of UV forcing with three functions *F(z)*. The sigmoidal fitting function seems to approximate with a good accuracy the trend of these values. Although noticeable dispersion, VIS forcings, and consequently VIS tropospheric information budget, seem to be not negligible. Considering the observed large noise levels and the need of accurately knowing surface albedo values, this sensitivity in Chappuis ozone bands can be exploited, in combination with UV information, to retrieve tropospheric ozone information from UV/VIS satellite data. An interesting parameter for our purposes is the ratio of the UV and VIS forcings above mentioned. In figure 4 the vertical trend of this quantity for our simulated data is depicted. Qualitatively the UV/VIS forcing ratio has a linear trend in the first height levels, and tend to saturate at a fixed value for z higher than 8 km. This behavior renders this parameter quite interesting for sounding the lower atmospheric heights, though uncertainties are large.

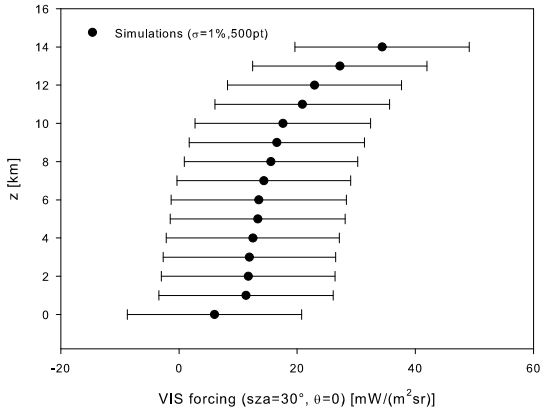

Figure 3. Dependence of VIS radiative forcing at fixed observation angle for ozone doubling, with height.

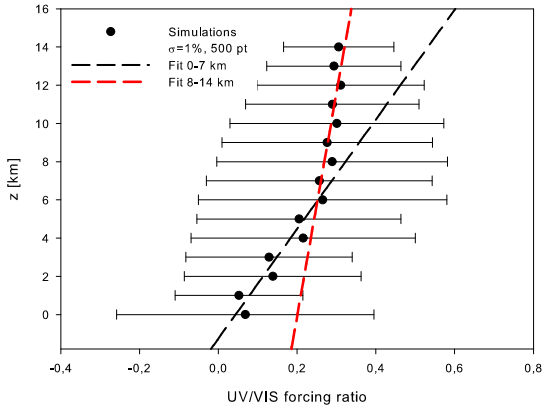

Figure 4. Dependence of UV/VIS forcing ratio with height. Two different fitting functions for the two height ranges 0-7 km and 8-14 km are reported.

From this simple exercise is possible to notice that a) the retrieval of height resolved information on tropospheric ozone is quite difficult owing to the low sensitivity, especially in the lower height levels and the large theoretical standard deviations, and b) the VIS range can however have an interesting role for this issue. NNs are particularly intended to work in cases of non-linear dependency between physical quantities. In some cases, weak dependencies can be found with the aid of NNs. From this point of view, this sensitivity analysis suggests a possible employment of such class of algorithms.

3. NNS FOR TOC RETRIEVALS FROM MODELLED UV/VIS SATELLITE DATA

Our first inversion exercise was referred to Tropospheric Ozone Column (TCO) retrieval; we plan to investigate the height resolved retrieval potentiality of our Nets in the future. We generated 4000 ozone profiles and we calculated correspondingly the Earth's radiance as described in the previous section, by means of the UVSPEC model. The tropopause has been considered in the range 14-17 km. The total ozone was varied between 350 and 250 DU. For part of the profiles, an additional contribution modelled by an exponential function to simulate ground production of ozone and some vertical transport has been considered. These modified profiles take the following simplified form:

$$O_3'(z) = O_3(z) + A \cdot e^{-\frac{z}{H}} \qquad (1)$$

The parameters A and H were varied in the ranges 1-4 the first, and 1-5 the second, respectively. A random value taken from a Gaussian distribution of mean value 0 and standard deviation 0.3 has been added to each A and H. These modified profiles and the non modified ones were also varied at all height levels adding a random value taken from a Gaussian distribution of mean value 0 and standard deviation the 50% of the considered concentration value. These operations have been made to generate a synthetic database of profiles and spectra, trying also to simulate, at some extent, cases of photochemical induced ozone generation in midlatitude summer urban environment. It has to be noticed that this dataset preparation doesn't pretend to model specific pollution phenomena with accuracy but is intended only to provide an extended dataset to investigate the inversion potentiality of our NNs.

The wavelength selection followed upon the sensitivity study of section 2. Our first experiment was made considering only the UV band; in a second stage we considered also the VIS band. We will pass to a discussion on the two approaches.

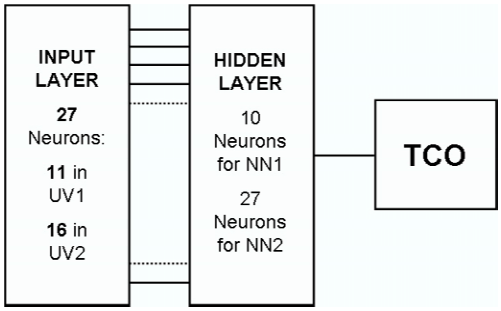

Figure 5. TOC NNs scheme. With NN1 and NN2 we intend that input radiance data is without or with a 1% additional noise.

3.1. Neural inversion with the UV spectral range

For this first approach two ranges were selected: the range of about 305.75-306.85 nm (NN UV1) and the range of about 322.05-324.30 nm (NN UV2). Both these bands are in the range of UV sensitivity resulting from the analysis of section 2; band NN UV1 in particular is in the interval of maximum sensitivity (see figure 1). The overall dataset has been split into two ensembles: the training and the test dataset. A crucial point of NNs development is the scaling of the input and output vectors to fit the optimal dynamical interval the neurons. Input data, in particular, needed care owing to the large intrinsic dynamics. From simulated Earth's radiance spectra it can be noticed that radiance values vary over more of an order of magnitude from NN UV1 to NN UV2. For this reason we performed a non linear scaling of the input vectors (bringing data in the interval ranging between -1 and 1), using the following expression 2.

$$NN_{\text{input}}(\text{RADIANCE}) = b \cdot \ln\left(-\frac{a}{\text{RADIANCE}} - 1\right) \qquad (2)$$

with a and b to be searched to fit the radiance values of the training dataset. It can be noticed how dynamics gained in the two regions of interest (near 0 for NN UV1 and near 55-60 mW/(m^{2}sr) for NN UV2). NNs have been tested also with input vector linear scaling; the accuracy results greatly improved with our non linear scaling. We chose as the output vector the TCO, calculated as the integration of the ozone concentration of our synthetic profiles in the range 0-14 km; output values have been linearly scaled to be in the range 0-1. We tried to invert the modelled spectra with (NN2) and without (NN1) the adding of a 1% noise to the radiance values. The first exercise can be viewed as an inversion of the radiative transfer model dedicated to TCO retrievals, while the second can be considered to take into account some source of noise due to UV/VIS sensor measurements. For both the approaches we chose to interpose a hidden layer between the input and the output. A schematic rationale of the NNs is showed in figure 5. We chose the dimension of the hidden layer by analyzing the retrieval error of the test dataset in function of the number of hidden neurons. We found that a minimum error value can be found for

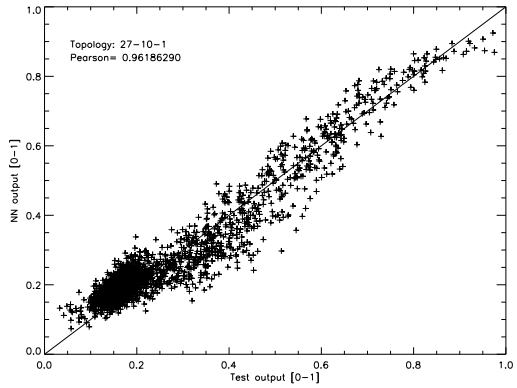

Figure 6. Scatterplot of TOC NN1 retrievals with true data (output vectors) for test datasets. Pearson coefficient value is reported.

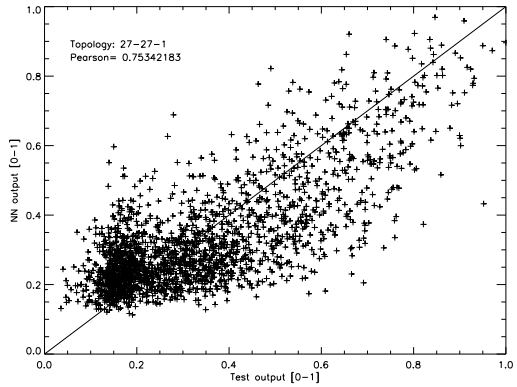

Figure 7. Scatterplot of TOC NN2 retrievals with true data (output vectors) for test datasets. Pearson coefficient value is reported.

10 and 27 neurons, respectively for NN1 and NN2. The learning function chosen was the Scale Conjugate Gradient (SCG) function, that allows shorter learning times with respect to the standard backpropagation scheme. In figures 6 and 7 the test datasets' retrievals are showed in a scatterplot that allows the comparison with the *true* values. The Pearson coefficients for the two comparisons are respectively 0.96 and 0.75. Such magnitude of correlation parameters, in relation to the little sensitivity of the Earth's radiation to tropospheric ozone, can be considered a surprisingly good result of NNs schemes.

3.2. Neural inversion with the UV/VIS spectral range

In the second stage of our work, we selected 28 UV/VIS wavelengths according to an extended pruning procedure performed as described in [9]. These selected wavelengths followed the underlying physics, with a high density in the UV and a distribution in the VIS strongly linked to the Chappuis band features. A schematic rationale of the NN is showed in figure 8. The NN obtained showed a surprisingly good retrieval power, enhancing of over 10% the correlation coefficient of the retrieved and the test TOC, with respect to UV-only case, on a test set of 1000 input-output pairs. In figure 9 the scatterplot of these data is reported.

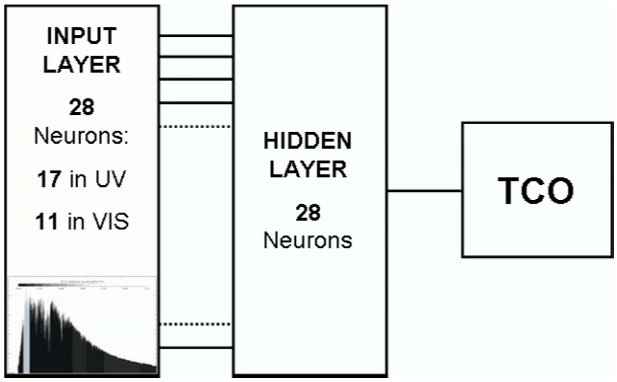

Figure 8. TOC UV/VIS NN rationale. The distribution of the selected wavelengths is depicted by the small figure in the first box; brighter areas are referred to spectral regions with higher densities (in terms of the number of selected wavelengths per nm).

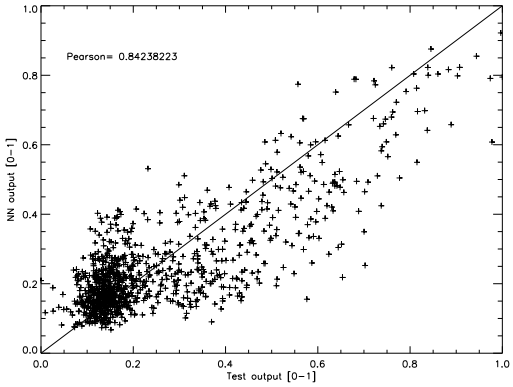

Figure 9. Scatterplot of TOC NN UV/VIS retrievals with true data (output vectors) for test datasets. Pearson coefficient value is reported.

3.3. Conclusions

In this paper we have reported some experiments on NNs based inversions of simulated ESA-Envisat SCIAMACHY UV/VIS radiance data, based upon a sensitivity study performed by means of the LibRadtran suite and of a complementary Extend Pruning process. The Nets demonstrated encouraging retrieval capabilities. In particular it was shown that the use of the VIS radiation in the Chappuis band can improve the retrieval capabilities of the NNs. Even if the results need more investigation, we'd like to stress that the procedure can easily be extended to the spectral measurements of the OMI instru-

ment, carried by the EOS-Aura platform; in this case, the improved horizontal resolution of the sensor could help in monitoring and understanding a number of local and short-range air pollution phenomena.

ACKNOWLEDGMENTS

Emanuele Angiuli is gratefully acknowledged for his valuable IDL advices. Special thanks to Andrea Minchella for logistic support.

REFERENCES

[1] Fishman, J., Watson, C.E., Larsen, J.C. & Logan, A. (1990) Distribution of tropospheric ozone determined from satellite data *J. Geophys. Res.* **95**(D4), 3599-3617.

[2] Chandra, S., Ziemke, J.R. & Martin, R.V. (2003) Tropospheric ozone at tropical and middle latitudes derived from TOMS/MLS residual: Comparison with a global model *J. Geophys. Res.* **108**(D9), doi:10.1029/2002JD002912.

[3] Ziemke, J.R., Chandra, S., Duncan, B.N., Froidevaux, L., Bhartia, P.K., Levelt P.F. & Waters, J.M. (2003) Tropospheric ozone determined from Aura OMI and MLS: Evaluation of measurements and comparison with the Global Modeling Initiative's Chemical Transport Model *J. Geophys. Res.* **111**, D19303, doi:10.1029/2006JD007089.

[4] Munro R., Siddans, R., Reburn, W.J. & Kerridge, B.J. (1998) Direct measurement of tropospheric ozone distributions from space" *Nature* **392**, 198-171.

[5] Liu, X., Chance, K., Sioris, C.E., Spurr, R.J.D., Kurosu, T.P., Martin, R.V. & Newchurch, M.J. (2005) Ozone Profile and Tropospheric Ozone Retrieval from Global Ozone Monitoring Experiment (GOME): Algorithm Description and Validation *J. Geophys. Res.* **110**(D20), D20307, doi:10.1029/2005JD006240.

[6] Del Frate, F., Ortenzi, A., Casadio, S. & Zehner, C. (2002) Application of neural algorithms for a real-time estimation of ozone profiles from GOME measurements *IEEE Trans. Geosci. Remote Sensing* **40**(10), 2263-2270.

[7] Müller, M.D, Kaifel, A.K., Weber, M., Tellmann, S., Burrows, J.P. & Loyola, D. (2003) Ozone profile retrieval from Global Ozone Monitoring Experiment (GOME) data using a neural network approach (Neural Network Ozone Retrieval SYstem (NNORSY)) *J. Geophys. Res.* **108**(D16), doi:10.1029/2002JD002784.

[8] Meijer, Y.J. et al. (2006) Evaluation of GOME ozone profiles from nine different algorithms *J. Geophys. Res.* **111,** D21306, doi:10.1029/2005JD006778.

[9] Del Frate, F., Iapaolo, M., Casadio, S., Godin-Beekmann, S. & Petitdidier, M. (2005) Neural networks for the dimensionality reduction of GOME measurement vector in the estimation of ozone profiles *J. Quant. Spectrosc. Radiat. Transf.* **92**, 275-291.

[10] Hornik, K., Stinchcombe, M. & White, H. (1989) Multilayer feedforward networks are universal approximators *Neural Networks* **2**(5), 359-366.

[11] Mayer, B. & Kylling, A. (2005) Technical note: The libRadtran software package for radiative transfer calculations - description and examples of use *Atmos. Chem. Phys.* **5**, 1855-1877.